



Phase coexistence in the mixed crystal  $\text{Rb}_{1-x}(\text{NH}_4)_x\text{H}_2\text{AsO}_4$   
by Nicholas Joaquim Pinto

A thesis submitted in partial fulfillment of the requirements for the degree of Doctor of Philosophy in  
Physics

Montana State University

© Copyright by Nicholas Joaquim Pinto (1992)

Abstract:

A study of the coexistence phenomenon in mixed crystals of rubidium ammonium dihydrogen arsenate has been done. Coexistence in this study refers to the simultaneous presence of ferroelectric and proton glass phases as temperature is lowered below the ferroelectric phase transition temperature  $T_c$ . Such coexistence is found to exist in these mixed crystals only for small ammonium concentrations. Our results show that coexistence exists for lower ammonium concentration than previously suggested. A study was also done on crystals with larger ammonium concentrations that show pure proton glass behavior and the results compared with the coexistence phenomenon.

Dielectric, spontaneous polarization and nuclear magnetic resonance experiments on mixed crystals with small ammonium concentrations show that at low temperatures there exists intimate coexistence of ferroelectric clusters with proton glass clusters below the glass transition temperature  $T_g$ . In the proton glass phase, we observe a spread of relaxation times due to the creation and annihilation of  $\text{HAsO}_4$  and  $\text{H}_3\text{AsO}_4$  pairs as they diffuse through the crystal. Spin lattice relaxation times for the acid deuterons in a 10% ammoniated sample show a broad  $T_1$  minimum near the glass transition temperature which is characteristic of proton glasses. Field-cooling experiments were also done on the pure proton glass. The results are consistent with dielectric measurements, but the remanent polarization was found to be extremely small. This polarization was found to depend on the rate of heating and cooling the sample while performing the experiment.

PHASE COEXISTENCE in the MIXED CRYSTAL  $\text{Rb}_{1-x}(\text{NH}_4)_x\text{H}_2\text{AsO}_4$

by

Nicholas Joaquim Pinto

A thesis submitted in partial fulfillment  
of the requirements for the degree

of

Doctor of Philosophy

in

Physics

MONTANA STATE UNIVERSITY  
Bozeman, Montana

November 1992

D378  
P6585

APPROVAL

of a thesis submitted by

Nicholas Joaquim Pinto

This thesis has been read by each member of the thesis committee and has been found to be satisfactory regarding content, English usage, format, citations, bibliographic style, and consistency, and is ready for submission to the College of Graduate Studies.

Nov. 4, 1992  
Date

V. Hugo Schmidt  
Chairperson, Graduate Committee

Approved for the Major Department

Nov 4, 1992  
Date

Hermann  
Head, Major Department

Approved for the College of Graduate Studies

11/17/92  
Date

R. Brown  
Graduate Dean

## STATEMENT OF PERMISSION TO USE

In presenting this thesis in partial fulfillment of the requirements for a doctoral degree at Montana State University, I agree that the Library shall make it available to borrowers under rules of the Library. I further agree that copying of this thesis is allowable only for scholarly purposes, consistent with "fair use" as prescribed in the U.S. Copyright Law. Requests for extensive copying or reproduction of this thesis should be referred to University Microfilms International, 300 North Zeeb Road, Ann Arbor, Michigan 48106, to whom I have granted "the exclusive right to reproduce and distribute copies of the dissertation in and from microfilm and the right to reproduce by abstract in any format."

Signature



Date

11-4-92

## ACKNOWLEDGEMENTS

I am very thankful to all the people in the physics department for their kindness and help during my stay as a graduate student at Montana State University. I sincerely thank my advisor Hugo Schmidt for his support and discussions that have given me a deeper understanding of hydrogen bonded ferroelectrics. To Toby Howell, thanks a million for teaching me the "nuts and bolts" of nuclear magnetic resonance, your assistance in helping me become an experimental physicist is greatly appreciated. I am also grateful to all the people who visited our lab, for their support and encouragement. Of special mention is George Tuthill, Jack Drumheller, Stuart Hutton (Stu) and Stefan Waplak.

Finally, I would like to thank Erik Andersen, Norm Williams and Mark Baldwin for their assistance and friendship.

## TABLE OF CONTENTS

	Page
1. INTRODUCTION.....	1
2. CRYSTAL GROWTH.....	15
Growth of RDA, chemical reaction.....	17
Growth of ADA, chemical reaction.....	18
Growth of RADA.....	18
3. APPARATUS AND EXPERIMENTS.....	20
Dielectric.....	20
Spontaneous Polarization.....	22
Field-Cooled and Zero-Field-Cooled.....	25
Nuclear Magnetic Resonance.....	28
4. THEORY.....	34
Proposed model to explain proton glass.....	35
Predicted phase diagram.....	41
5. RESULTS AND DISCUSSION.....	43
Dielectric Measurements.....	43
Curie-Weiss Law.....	50
Characteristic features of Proton Glass.....	52
Comparison of coexistence with pure glass.....	57
Cole-Cole plots.....	58
Spontaneous Polarization Measurements.....	64
Landau free energy expansion.....	65
Comparison of spontaneous polarization of mixed and pure crystals.....	66
Field Cooling Measurements.....	76
Susceptibility at heating and cooling rate of 1 K/min.....	79
Susceptibility at heating and cooling rate of 4 K/min.....	80

## TABLE OF CONTENTS - Continued

	Page
Nuclear Magnetic Resonance.....	83
Ammonium deuteron spectra.....	85
Spin lattice relaxation times for ND <sub>4</sub> <sup>+</sup> deuterons.....	88
Spin lattice relaxation times for acid deuterons.....	89
6. CONCLUSIONS.....	92
Recommendations for further work.....	95
REFERENCES CITED.....	97
APPENDIX.....	100

## LIST OF TABLES

Table	Page
1. Tabulated temperatures of various activation energies mentioned in the text including the activation energies responsible for dielectric relaxation. These results (except for the activation energy) are obtained by analyzing the data taken at 1 kHz.....	48
2. Tabulated values of $\beta$ and $\gamma$ defined in Eq. (5.3) for RDA and DRDA together with parameters defined in the text.....	68

## LIST OF FIGURES

Figure	Page
1. Phase diagram of RADA mixed crystals as a function of ammonium concentrations ( $x$ ) and temperature. PE, FE, PG and AFE denote paraelectric, ferroelectric, proton glass and antiferroelectric phases respectively.....	2
2. The crystal structure of KDP at room temperature..	5
3. $c$ -axis projection of KDP in the ferroelectric phase.....	6
4. Schematic representation of the dipole moment in KDP. Polarization along the $c$ axis.....	8
5. Structure of a mixed crystal of RADA showing a $\text{NH}_4^+$ ion that replaced a Rb atom along the $c$ axis. A $\text{NH}_4^+$ at height 0 is shown attached to nearby oxygens of a $\text{AsO}_4$ tetrahedra. The heights in units of $c$ of the arsenate centers of the $\text{AsO}_4$ tetrahedra are indicated. The offcenter motion of the ammonium ion is indicated by the arrow. This results in the formation of two long and two short bonds with the surrounding $\text{AsO}_4$ tetrahedra...	9
6. Schematic representation of the antiferroelectric phase of ADP.....	10
7. (a) Sawyer-Tower bridge for spontaneous polarization measurements (b) Saturated hysteresis loop showing the voltages used to calculate the spontaneous polarization and coercive field.....	23
8. Circuit diagram used for field-cooling experiments.	26
9. Block diagram of the NMR spectrometer.....	29
10. Quadrupolar splitting in deuterated KDP. Deuteron resonant frequencies vs. $\Theta_z$ .....	32
11. Transition temperature $T_g$ versus the ratio $\Omega/J_0^{\text{AA}}$ for $x_A=x_B=0.5$ .....	40

## LIST OF FIGURES - Continued

Figure	Page
12. Calculated phase diagram for RADP showing the stability limits of the paraelectric phase with respect to a freezing into the ferro-, antiferroelectric and proton glass phases.....	41
13. The partial phase diagram of RADA as a function of fractional ammonium concentration $x$ and temperature $T$ . PE, FE, PG, F-P and F-G denote paraelectric and ferroelectric phases, proton glass regime, mixed ferroelectric-paraelectric and ferroelectric-proton glass phases respectively. The dotted line represents extension from this work. The solid squares represent data from this work; other symbols represent data from Trybula <i>et al.</i> (Ref. 4a).....	44
14. Temperature dependence of the real part of the dielectric constant $\epsilon_a'$ measured along the $a$ axis for various ammonium concentrations $x$ in RADA. Solid line represents a fit to Eq.(4.1); see Table 1 for fitting constants.....	46
15. Temperature dependence of the real part of the dielectric constant $\epsilon_a'$ measured along the $a$ axis for various ammonium concentrations $x$ in DRADA. Solid line represents a fit to Eq.(4.1); see Table 1 for fitting constants.....	47
16. Temperature dependence of the (a) imaginary part $\epsilon_a''$ and (b) real part $\epsilon_a'$ of the dielectric permittivity in the proton glass regime for $x=0.05$ RADA. Solid lines are guides to the eye.....	52
17. Temperature dependence of the (a) imaginary part $\epsilon_a''$ and (b) real part $\epsilon_a'$ of the dielectric permittivity in the proton glass regime for $x=0.05$ DRADA. Solid lines are guides to the eye....	53
18. Temperature dependence of the (a) imaginary part $\epsilon_a''$ and (b) real part $\epsilon_a'$ of the dielectric permittivity in the proton glass regime for $x=0.10$ RADA. Solid lines are guides to the eye.....	54

## LIST OF FIGURES - Continued

Figure	Page
19. Temperature dependence of the (a) imaginary part $\epsilon_a''$ and (b) real part $\epsilon_a'$ of the dielectric permittivity in the proton glass regime for $x=0.10$ DRADA. Solid lines are guides to the eye....	55
20. Cole-Cole plots for $x=0.10$ RADA in the proton glass region. The symbols represent the same frequencies as in Figs. 18 and 19. Solid lines represents fits to the equation of a circle.....	58
21. Cole-Cole plots for $x=0.10$ DRADA in the proton glass region. The symbols represent the same frequencies as in Figs. 18 and 19. Solid lines represents fits to the equation of a circle.....	59
22. Temperature dependence of the (a) real part $\epsilon_a'$ and (b) imaginary part $\epsilon_a''$ of the dielectric permittivity measured along the <u>a</u> axis in the proton glass regime for $x=0.40$ RADA.....	61
23. Temperature dependence of the (a) real part $\epsilon_a'$ and (b) imaginary part $\epsilon_a''$ of the dielectric permittivity measured along the <u>a</u> axis in the proton glass regime for $x=0.28$ DRADA.....	62
24. Temperature dependence of the (a) real part $\epsilon_a'$ and (b) imaginary part $\epsilon_a''$ of the dielectric permittivity measured along the <u>c</u> axis in the proton glass regime for $x=0.28$ DRADA.....	63
25. Spontaneous polarization obtained from saturated hysteresis loops in RDA ( $x=0$ ; $\circ$ ) and RADA ( $x=0.08$ ; $\triangle$ ) as a function of temperature. The open diamond symbol represents spontaneous polarization obtained from Eq. (5.4) and Fig. 27. for RADA $x=0.08$ .....	66
26. Real part of the dielectric permittivity $\epsilon_a'$ at 1 kHz as a function of temperature along the <u>c</u> axis, ( $\circ$ ) for RDA and ( $\triangle$ ) for DRDA. Solid line represents a fit to the Curie-Weiss law of Eq. (5.1).....	67

## LIST OF FIGURES - Continued

Figure	Page
27. Real part of the dielectric permittivity $\epsilon_a'$ for the undeuterated mixed crystals at 1 kHz as a function of temperature along the <u>a</u> axis. $\epsilon_\infty'$ is assumed to be 10.....	70
28. Spontaneous polarization obtained from saturated hysteresis loops in DRDA ( $x=0$ ; $\circ$ ) and DRADA ( $x=0.08$ ; $\triangle$ ) as a function of temperature. The open diamond symbol represents spontaneous polarization obtained from Eq. (5.4) and Fig. 29 for DRADA $x=0.08$ .....	72
29. Real part of the dielectric permittivity $\epsilon_a'$ for the deuterated mixed crystals at 1 kHz as a function of temperature along the <u>a</u> axis. $\epsilon_\infty'$ is assumed to be 10.....	73
30. Temperature dependence of the field-cooled ( $\circ$ ) and zero-field-cooled ( $\bullet$ ) static dielectric constant (left scale) of DRADA with $x=0.28$ measured along the <u>a</u> axis. The remanent polarization $P_R$ ( $\diamond$ ) is also shown (right scale). The electric field applied was 500 V/cm and the heating/cooling rate was 1 K/min.....	79
31. Temperature dependence of the field-cooled ( $\circ$ ) and zero-field-cooled ( $\bullet$ ) static dielectric constant (left scale) of DRADA with $x=0.28$ measured along the <u>a</u> axis. The remanent polarization $P_R$ ( $\diamond$ ) is also shown (right scale). The electric field applied was 500 V/cm and the heating/cooling rate was 4 K/min.....	80
32. Temperature dependence of the $ND_4^+$ deuteron spectra. $T_c$ for this sample is 146 K. Note the gradual build up of the broad component due to the ferroelectric phase.....	85
33. $1/T_1$ versus temperature for the ammonium deuterons in DRADA ( $x=0.10$ ). The minimum in this case is driven by the reorientations of the ammonium deuterons.....	88

## LIST OF FIGURES - Continued

Figure	Page
34. $1/T_1$ versus temperature for the acid deuterons in DRADA ( $x=0.10$ ). Note that three $T_1^{-1}$ minima are observed in this system. The first minimum is due to interbond motion and the third is due to extreme slowing down of the deuterons in the O-D...O bond.....	89

## ABSTRACT

A study of the coexistence phenomenon in mixed crystals of rubidium ammonium dihydrogen arsenate has been done. Coexistence in this study refers to the simultaneous presence of ferroelectric and proton glass phases as temperature is lowered below the ferroelectric phase transition temperature  $T_c$ . Such coexistence is found to exist in these mixed crystals only for small ammonium concentrations. Our results show that coexistence exists for lower ammonium concentration than previously suggested. A study was also done on crystals with larger ammonium concentrations that show pure proton glass behavior and the results compared with the coexistence phenomenon.

Dielectric, spontaneous polarization and nuclear magnetic resonance experiments on mixed crystals with small ammonium concentrations show that at low temperatures there exists intimate coexistence of ferroelectric clusters with proton glass clusters below the glass transition temperature  $T_g$ . In the proton glass phase, we observe a spread of relaxation times due to the creation and annihilation of  $\text{HAsO}_4$  and  $\text{H}_3\text{AsO}_4$  pairs as they diffuse through the crystal. Spin lattice relaxation times for the acid deuterons in a 10% ammoniated sample show a broad  $T_1$  minimum near the glass transition temperature which is characteristic of proton glasses. Field-cooling experiments were also done on the pure proton glass. The results are consistent with dielectric measurements, but the remanent polarization was found to be extremely small. This polarization was found to depend on the rate of heating and cooling the sample while performing the experiment.

## CHAPTER 1

## INTRODUCTION

Investigation of the proton glass rubidium ammonium dihydrogen arsenate ( $\text{Rb}_{1-x}(\text{NH}_4)_x\text{H}_2\text{AsO}_4$ -RADA) and its deuterated counterpart ( $\text{Rb}_{1-x}(\text{ND}_4)_xD_2\text{AsO}_4$ -DRADA) has been carried out to understand the coexistence of ferroelectric and proton glass phases as temperature is lowered below the ferroelectric transition temperature  $T_c$ . Above this temperature the system is in the paraelectric phase. Below the transition temperature, for  $x=0$  the system is ferroelectric below  $T_c$  and for  $x=1$  the system is antiferroelectric below the Néel temperature  $T_N$ . For a range of intermediate  $x$ -values shown in the phase diagram in Fig. 1, the system makes a smooth transition to the "proton glass" phase. This "transition" to the glassy phase is not a thermodynamic phase transition. Rather, it is an effect seen due to competing ferroelectric and antiferroelectric interactions as a frequency dependent freezing of protons in their bond sites as temperature is lowered. The region on the phase diagram where one observes a dispersion in the

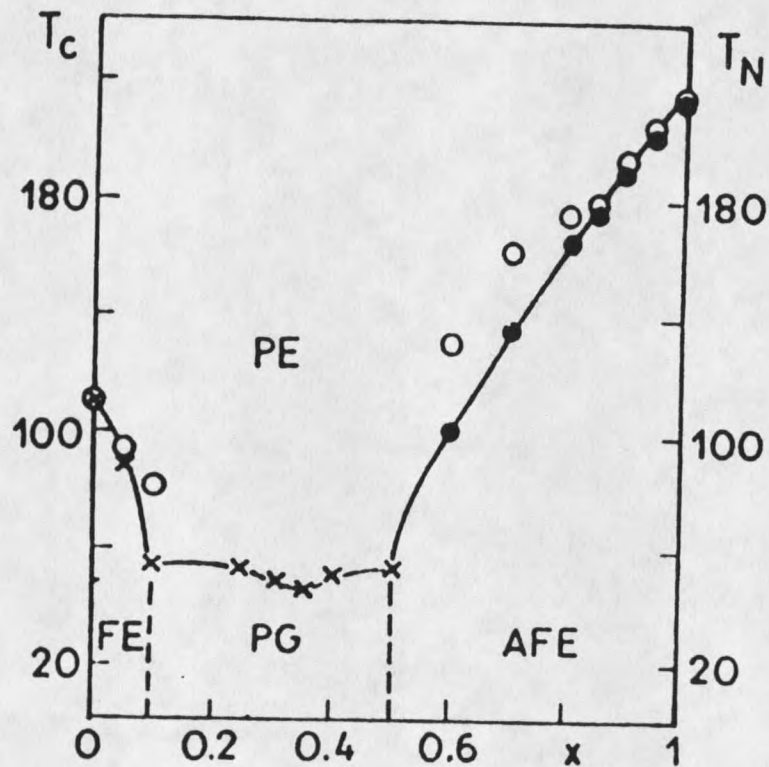


Figure 1. Phase diagram of RADA mixed crystals as a function of ammonium concentrations ( $x$ ) and temperature. PE, FE, PG and AFE denote paraelectric, ferroelectric, proton glass and antiferroelectric phases respectively.<sup>[1]</sup>

dielectric response is called the "proton glass" phase. Such a phase diagram shows the boundaries between the paraelectric (PE) and ferroelectric (FE) phase for small ammonium (x) concentrations and the boundary between the PE and antiferroelectric (AFE) phase for large x values. Our experiments concentrate on crystals having ammonium concentrations (x) close to the ferroelectric side of the phase diagram.

Proton glass was first discovered by E. Courtens<sup>[2]</sup> in 1982 in the mixed crystal rubidium ammonium dihydrogen phosphate (RADP) with  $x=0.34$ . In this system, the frustration that leads to glassy behavior results from the random placement of the  $\text{NH}_4^+$  cation. To understand the role of the  $\text{NH}_4^+$  cation, it is important to understand the origin of ferroelectricity and antiferroelectricity in the pure crystals. The most widely studied ferroelectric crystal in this family of crystals is  $\text{KH}_2\text{PO}_4$  (KDP). In the case of the antiferroelectric crystals it is  $(\text{NH}_4)\text{H}_2\text{PO}_4$  (ADP). In the crystals studied here the following substitution must be made, Rb for K and As for P. The procedure used to grow these crystals is given in Chapter 2. These crystals are tetragonal in their structure with the ferroelectric or antiferroelectric axis along the  $c$  direction of the crystal.

Fig. 2 shows the crystal structure of KDP<sup>[3]</sup> at room

temperature and Fig. 3 is its  $c$ -axis projection in the ferroelectric ordered phase.<sup>[4]</sup> The structure consists of two interpenetrating sublattices. One is a body-centered sublattice of  $\text{PO}_4$  tetrahedra and the other a body-centered sublattice of  $\text{K}^+$  ions. The  $\text{K}^+$  and  $\text{P}^{5+}$  ions are alternately arranged in chains running along the  $c$  axis and are spaced from each other by a distance  $c/4$ . Each phosphorus ion is surrounded by four oxygen ions at the corners of a tetrahedron and each  $\text{PO}_4$  group is hydrogen bonded to four other  $\text{PO}_4$  groups via 'acid' hydrogen bonds. Because these  $\text{PO}_4$  neighbors in adjacent chains are  $c/4$  higher or lower than the  $\text{PO}_4$  in question, the linkage is such that there is an  $\text{O}\dots\text{H}-\text{O}$  'acid' hydrogen bond between the one 'upper oxygen' of one  $\text{PO}_4$  group and one 'lower oxygen' of a  $\text{PO}_4$  group spaced  $c/4$  above the previous one. These hydrogen bonds are nearly perpendicular to the  $c$  axis. Neutron diffraction studies show that only two hydrogen atoms are located near a  $\text{PO}_4$  group making it as a whole an  $(\text{H}_2\text{PO}_4)^-$  ion. Neutron diffraction studies also show that the hydrogen atoms are statistically distributed at the center of the  $\text{O}-\text{H}\dots\text{O}$  bonds in the paraelectric phase while in the ferroelectric phase the protons are statistically off center in the hydrogen bond. In this phase, the protons are ordered in such a way that in a single domain the protons are either close to the 'upper oxygen' or 'lower oxygen'

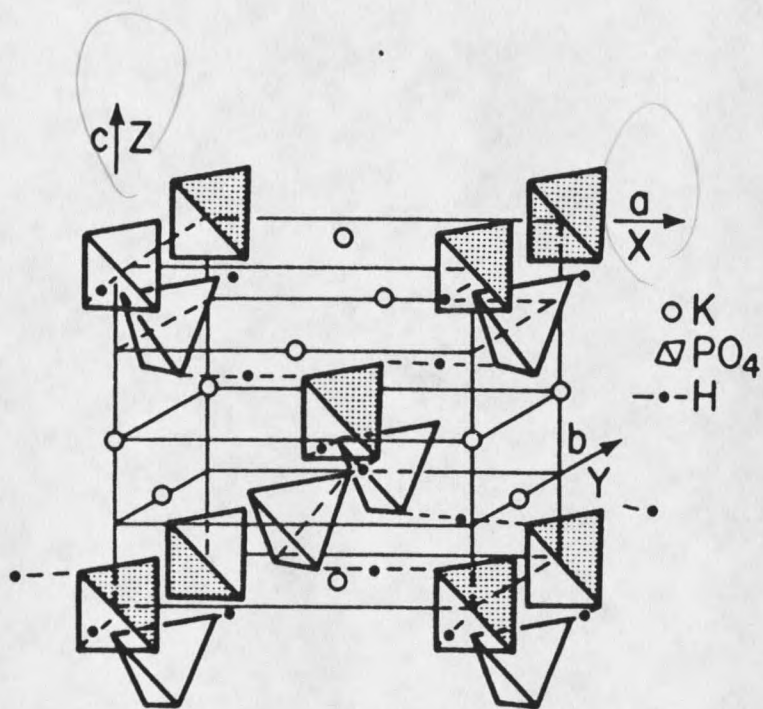


Figure 2. The crystal structure of KDP at room temperature.<sup>[3]</sup>

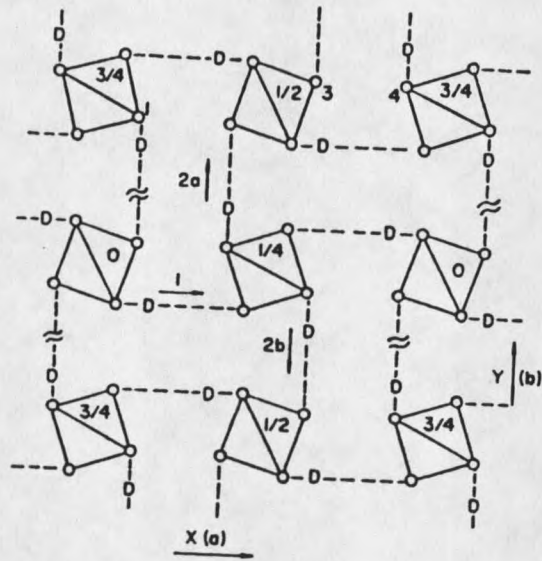


Figure 3.  $c$ -axis projection of KDP in the ferroelectric phase.<sup>[4]</sup>

depending on the polarity. This ordering effect of the protons around the  $PO_4$  tetrahedron is the key factor responsible for ferroelectricity in these crystals. In this ordered state the polarization arises from the displacements of  $K^+$  and  $P^{5+}$  ions in the direction of the  $c$  axis as shown in Fig. 4. The direction of the spontaneous polarization is along the  $P^{5+}$  displacement. Thus, when the polarization is 'up', these protons are nearest to the 'lower oxygen' ions of each  $PO_4$  group and vice versa.

The antiferroelectric counterpart has  $NH_4^+$  substituted for  $K^+$  and as a result the 'ammonium' protons are hydrogen bonded to the oxygens in addition to the 'acid' protons. Two of the 'ammonium' protons form 'short' bonds with the surrounding  $PO_4$  tetrahedra and two 'long' as seen in Fig. 5. This has an influence on the position of the 'acid' proton in its  $O-H...O$  bond. In the antiferroelectric phase the arrangement of the 'acid' protons is such that each  $PO_4$  tetrahedron has a proton at the upper and at the lower end unlike in KDP where in the ferroelectric phase all the 'acid' protons were attached either to the top or bottom of the  $PO_4$  tetrahedron. Such an arrangement of the protons results in the polarization alternately pointing in the 'up' and 'down' directions as seen in Fig. 6 yielding a net polarization of zero. The arrows indicate the direction of polarization in a unit cell.

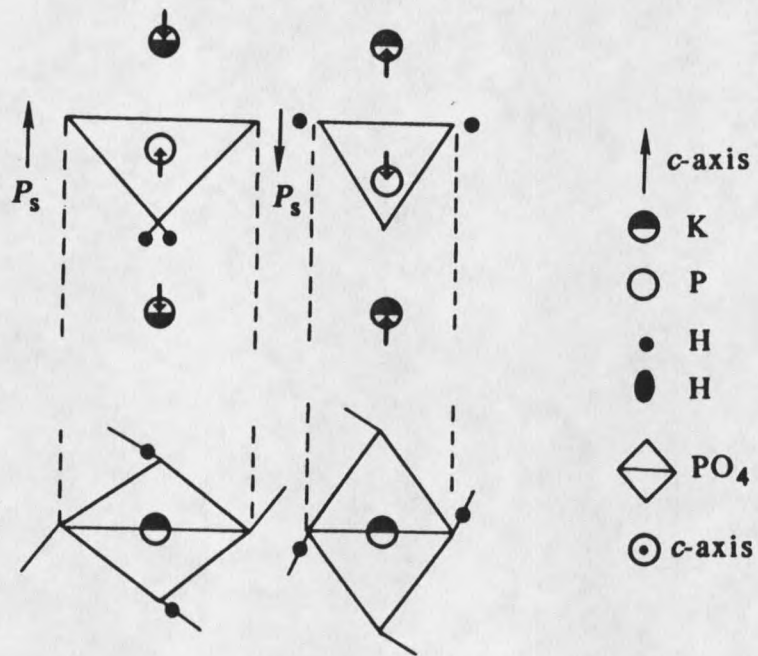


Figure 4. Schematic representation of the dipole moment in KDP. Polarization along the  $c$  axis.<sup>[5]</sup>



























































































































































































